

Satellite Based Surface Solar Irradiance Retrieval

Attilio Gambardella*, Thomas Huld and Jean Verdebout

¹ Joint Research Centre of the European Commission - Via E.Fermi 2749, I-21027 Ispra (VA), Italy.y

* Corresponding Author, attilio.gambardella[at]jrc.ec.europa.eu

Abstract

A new scheme for solar irradiance retrieval for the Europe from MSG data is here proposed. The surface irradiance is obtained by interpolation of multidimensional LUT relating surface irradiance to set of input parameters. The LUT is generated using the radiative transfer code libRadtran for a variety of atmospheres and cloud conditions. The validation of the irradiance retrieval scheme is based on set of 25 ground stations with measurements of global solar irradiance.

1. Introduction

Accurate solar radiation data derived from satellite data, such as Meteosat Second Generation (MSG) or GOES, will significantly improve most advanced solar energy applications like grid integration of photovoltaics, control of solar thermal power plants, future irradiance forecasting schemes, etc. Solar irradiance schemes using weather satellites provide accurate solar irradiance data with a high spatial and temporal and constitute a powerful alternative to a meteorological ground network for both climatological and operational data for solar resource assessment [1]. It is expected that these new products will establish the primary solar radiation data source in the future and the expensive use of ground based pyranometer networks will be restricted to special investigations and high quality reference measurements at selected sites.

Different methods exist to derive the solar surface irradiance from satellite data. A first class of methods, mainly used for data from geostationary satellites, uses normalized reflectance measurements to determine the cloud transmission or cloud index. A clear sky model is used afterwards to calculate the solar surface irradiance based on the retrieved cloud index. One example for this type of methods is the Heliosat method [2]-[3]. Another type of method relates top of atmosphere reflected radiation flux density to the solar irradiance at the surface. One prominent and widely used approach in this class is the method of Pinker and Laszlo [4], which uses look-up tables (LUT) for the retrieval of solar surface irradiance. In the last years new generations of retrieval schemes are based on Radiative Transfer Model (RTM) algorithms [5]. The main motivation for such trend is that RTM based retrieval algorithms have the potential to exploit the increased information on the atmospheric state, ranging from new satellite systems to improvements in numerical weather prediction analysis data. However, it must be noted that for operational processing a high computing performance of the algorithm is a pre-requisite. As a consequence of the above mentioned aspects, a new scheme for solar irradiance retrieval for the Europe from MSG data is here proposed.

2. The Retrieval Scheme

The proposed scheme to derive solar irradiance is based on the approach proposed by Verdebout [6]. The calculation scheme, originally developed for UV irradiance, is adapted for calculation of shortwave radiation from MSG satellite data. According to this scheme the surface irradiation is obtained by interpolation of multidimensional LUT relating surface irradiance to set of input parameters. The LUT is generated using the radiative transfer code libRadtran [7] for a variety of atmospheres and cloud conditions described by total ozone column amount, near surface horizontal visibility, effective surface albedo, cloud optical thickness and atmospheric water vapor. The horizontal visibility is used to approximate the atmospheric optical depth and was derived on daily basis from 1000 meteorological stations over Europe. The variability of water vapor is simplified to one constant value. In addition to these parameters, the LUT describes surface irradiance for a range of surface elevations and solar zenith angles.

The cloud optical thickness as estimate of radiation attenuation by clouds is derived from MSG data using a second LUT that simulates the “at sensor radiance”. The actual cloud optical thickness is calculated by inversion of LUT, and interpolation between pre-calculated values for the actual image digital count, effective surface albedo and solar and satellite geometry. In this approach, the lowest value in 30-days image stack is used to calculate effective surface albedo for snow-free pixel. The algorithm also accounts for reverse response of image digital counts to increasing cloud thickness at pixels with high effective surface albedo, e.g. snow. For snow detection algorithm, additional spectral bands from middle infrared and thermal bands of MSG instrument are used. The results of this model are layers of shortwave irradiance with spatial resolution of 3 arc minutes in 15 minutes time step (see Fig.1).

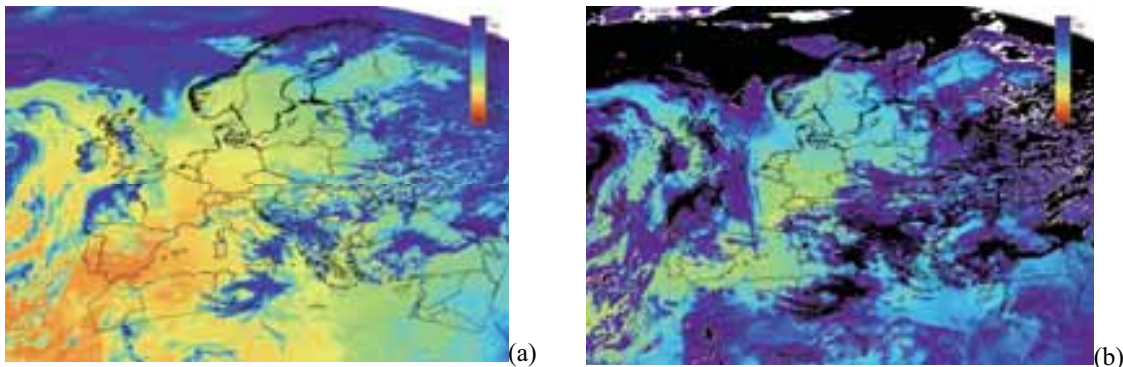


Fig.1: retrieved Global Horizontal (a) and Direct Horizontal (b) components relevant to the MSG data set acquired on 01 June 2005 12:00 GMT. Data are in WGS84 coordinate system. Extent is 20:00W 48:00E 25:00S 73:00N. Resolution is 00:03 (0.05deg).

3. Validation

3.1. Ground measurement data

Evaluation of retrieval scheme is based on set of 25 ground stations with measurements of global solar irradiance for year 2005. Most of the stations are from high quality measurements networks: International Daylight Measurement Programme (IDMP), Baseline Surface Radiation Network

(BSRN), and World Radiation Data Centre (WRDC). The time step of measurements data ranges from 1 to 60 min. All data have been subject of quality checking procedures and all erroneous data were excluded from analysis. The map of stations is on the Fig.2.

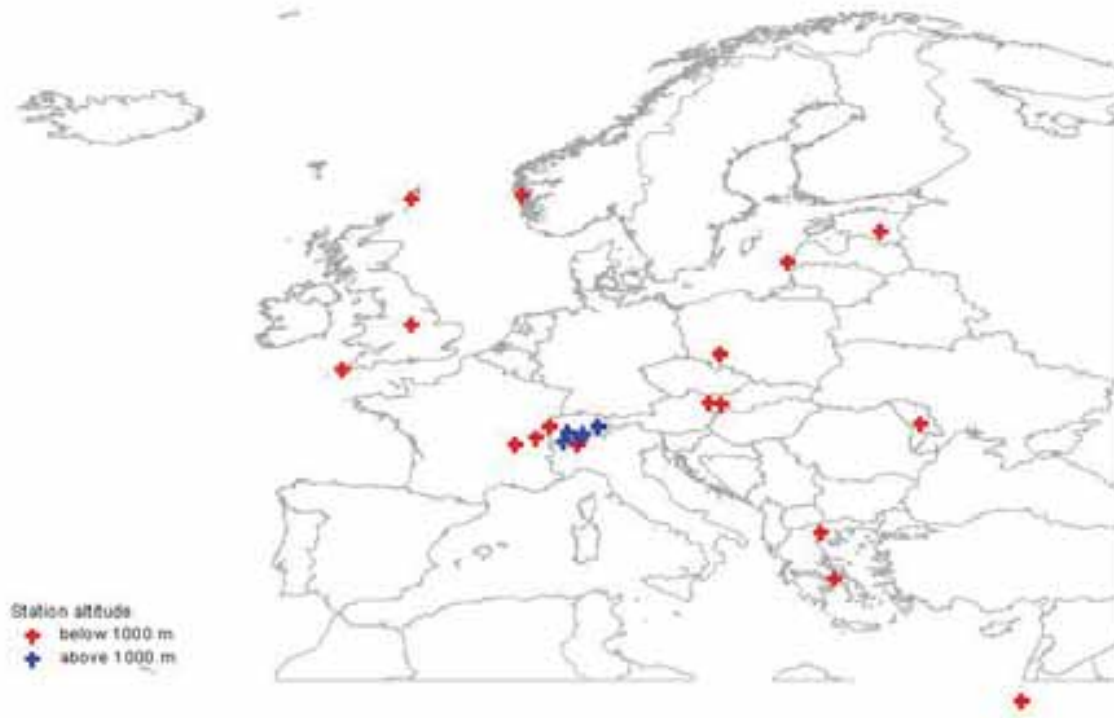


Fig. 2: Ground measurements stations used in model.

3.2. Retrieval scheme assessment methods

Following first order statistical measures are used for analysis of retrieval scheme performance [10]-[11]: mean bias difference (MBD), mean absolute difference (MAD), root mean squared difference (RMSD), correlation coefficient (CC); and corresponding relative measures: relative mean bias difference (rMBD), relative mean absolute difference (rMAD), relative root mean squared difference (rRMSD).

Due to differences in time step of measurements and existence of missing data gaps the data were harmonized prior to use for comparison. Because most of the ground measurements are available only in 60 min time step, this interval has been used for the comparison of all data sets. Time of the ground measurements has been shifted to represent centres of the measurements integration interval. Measurements from datasets with shorter time step have been downsampled into 60 min intervals. Then for each ground measurements time record satellite model outputs (with 15 min step) have been averaged. Only data with minimum number of three valid model records in given hour are considered as sufficient, otherwise no data flag are used for given hour record. Scan time offset of satellite data has been taken into consideration as well.

Subsequently, ground measurements and satellite retrieval scheme datasets have been compared and all records having no data values at least in one of the dataset have been excluded from the analysis. In addition to the hourly data, an analysis of model performance for daily and monthly values has been performed as well. In this case daily values are derived as an integration of all valid hourly values. Same approach was used for monthly values. It is important to note that integrated values do not represent total irradiance at the site because of either measurements or model data gaps.

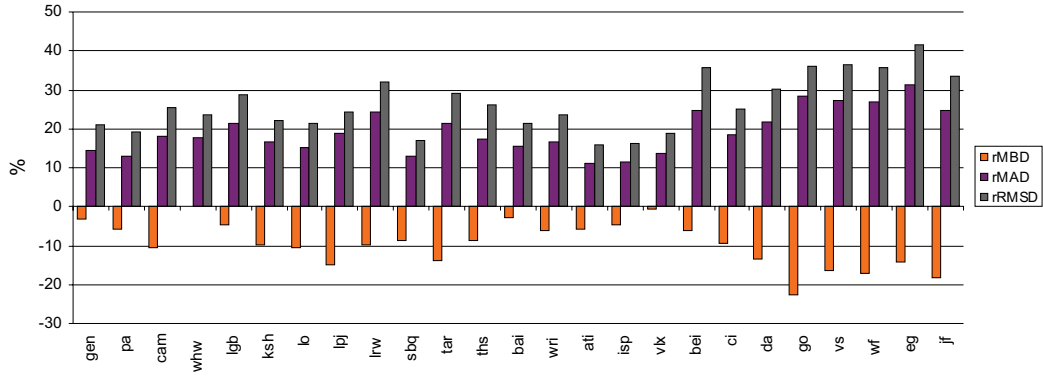
3.3. Hourly statistics of the satellite retrieval scheme performance

The retrieval scheme outputs show negative bias for all analyzed stations. Mean bias difference is smallest for the Wien, Vaulx un Velin, Bratislava, Geneve, Loughborough and Ispra. For the rest of sites the negative bias exceeds -5 %. See tab. 1 and Fig. 3. All errors increase with site altitude, for Alpine sites above 2500m the errors are twice as large as those in low altitudes below 500m (Fig. 4). There is no latitudinal trend in bias, but rMAD and rRMSD show increase of error with latitude (Fig. 5), that is probably related to higher uncertainty in modeling of more variable cloud pattern present in high latitudes. In middle latitudes the spread of errors is high, higher values are mostly from sites at high altitudes.

Tab. 1: The summary results of the satellite retrieval scheme performance on hourly basis.

station	db table	longitude	latitude	elev	MBD	MAD	RMSD	CC	rMBD	rMAD	rRMSD
Geneve	gen_r_gen_60min	6.132	46.200	420	-11.3	49.2	71.4	0.962	-3.3	14.5	21.1
Payerne	pa_r_pa_60min	6.943	46.814	490	-23.7	53.0	78.8	0.955	-5.8	12.9	19.2
Camborne	cam_r_cam_60min	-5.317	50.217	88	-31.1	54.1	76.0	0.954	-10.4	18.2	25.5
Wien_hohe_warte	whw_r_whw_60min	16.356	48.249	203	-0.1	54.8	73.9	0.956	0.0	17.5	23.7
Loughborough	lgb_r_lgb_01min	-1.230	52.770	70	-11.4	52.9	71.8	0.940	-4.6	21.2	28.8
Kishinev	ksh_r_ksh_60min	28.816	47.001	205	-34.8	57.8	77.9	0.962	-9.9	16.4	22.1
Locarno-Monti	lo_r_lo_60min	8.787	46.173	370	-39.9	57.4	80.8	0.966	-10.6	15.3	21.5
Liepaja_rucava	lpj_r_lpj_60min	21.017	56.483	4	-43.3	54.8	71.0	0.970	-14.8	18.7	24.3
Lerwick	lrw_r_lrw_60min	-1.183	60.133	84	-22.5	56.4	74.0	0.925	-9.7	24.4	31.9
Sde Boqer	sbq_r_sbq_60min	34.767	30.767	457	-50.8	76.0	100.4	0.954	-8.6	12.9	17.1
Tartu_toravere	tar_r_tar_60min	26.466	58.265	70	-40.1	61.2	83.1	0.943	-14.0	21.4	29.0
Thessaloniki	ths_r_ths_60min	22.959	40.632	60	-37.8	76.0	114.5	0.919	-8.6	17.2	26.0
Bratislava	bai_r_bai_01min	17.071	48.169	195	-9.2	48.7	67.3	0.965	-2.9	15.5	21.4
Wroclaw	wri_r_wri_01min	17.014	51.126	111	-18.7	50.8	72.1	0.960	-6.1	16.5	23.5
Athens	ati_r_ati_01min	23.718	37.972	107	-26.3	51.3	72.7	0.970	-5.7	11.2	15.9
Ispra	isp_r_isp_01min	8.627	45.812	220	-16.5	39.8	57.4	0.977	-4.7	11.4	16.4
Vaulx un Velin	vlx_r_vlx_01min	4.922	45.779	170	-2.5	46.1	63.0	0.971	-0.7	13.8	18.9
Bergen	bei_r_bei_60min	5.332	60.384	45	-13.1	52.7	76.3	0.923	-6.1	24.6	35.6
Cimetta	ci_r_ci_10min	8.790	46.201	1670	-36.1	69.5	94.9	0.945	-9.6	18.4	25.1
Davos	da_r_da_60min	9.844	46.813	1610	-50.3	79.9	111.5	0.922	-13.6	21.6	30.1
Gornergrat	go_r_go_10min	7.785	45.984	3110	-104.7	130.3	166.5	0.886	-22.7	28.3	36.1
SLF Versuchsfeld	vs_r_vs_10min	9.809	46.828	2540	-63.4	104.4	139.6	0.875	-16.5	27.3	36.4
Weissfluhjoch	wf_r_wf_10min	9.805	46.833	2690	-66.1	104.3	138.3	0.876	-17.1	27.0	35.9
Eggishorn	eg_r_eg_10min	8.927	46.427	2895	-57.3	125.6	166.6	0.801	-14.3	31.3	41.5
Jungfraujoch	jf_r_jf_60min	7.985	46.549	3580	-81.5	111.3	149.7	0.893	-18.2	24.8	33.4

Gh sat. model: relative hourly differences (2005)



Gh sat. model: absolute hourly differences (2005)

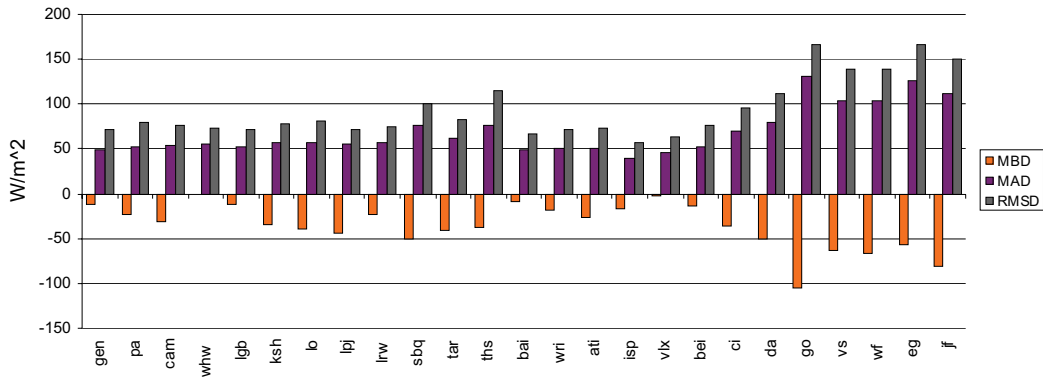


Fig. 3. a) first order relative statistic measures of hourly values of global irradiance and b) their absolute counterparts.

Model error vs. altitude

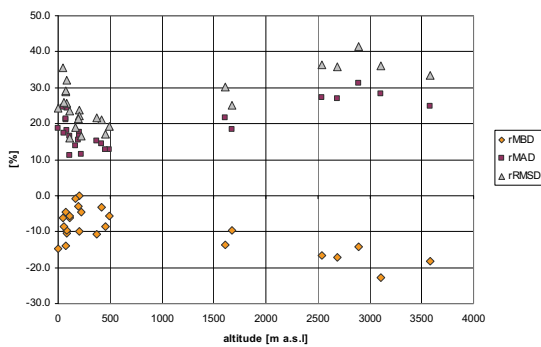


Fig. 4. Model errors dependence on site altitude.

Model error vs. latitude

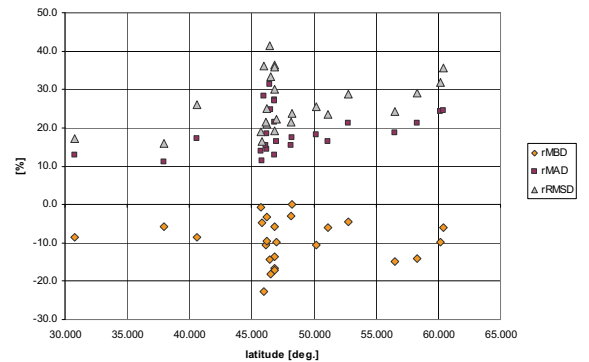


Fig. 5. Model errors by site latitude.

3.4. Daily statistics of the satellite retrieval scheme performance

Daily accuracy closely follows trends of hourly accuracies (see tab. 2). High negative bias was preserved, rMAD and rRMSD decreased with integrating diurnal variability into one value, thus removing errors arising from instantaneous (hourly) model outputs (see fig. 6). Fig. 6 shows, that only 15-35% of hourly errors is result of a high frequency instantaneous variability, and remaining 65-85% of the error is caused by integrated daily differences.

Tab. 2: The summary results of the satellite retrieval scheme performance on daily basis.

station	db	table	longitude	latitude	elev	MBD	MAD	RMSD	CC	rMBD	rMAD	rRMSD
Geneve	gen	r_gen_60min	6.132	46.200	420	-112.6	322.4	435.1	0.988	-3.3	9.5	12.9
Payerne	pa	r_pa_60min	6.943	46.814	490	-191.4	299.8	429.0	0.989	-5.8	9.0	12.9
Camborne	cam	r_cam_60min	-5.317	50.217	88	-306.1	382.5	508.8	0.982	-10.4	13.1	17.4
Wien_hohe_warte	whw	r_whw_60min	16.356	48.249	203	-0.8	324.0	407.8	0.988	0.0	11.4	14.4
Loughborough	lgb	r_lgb_01min	-1.230	52.770	70	-109.5	336.1	439.3	0.977	-4.6	14.0	18.3
Kishinev	ksh	r_ksh_60min	28.816	47.001	205	-316.7	366.4	466.7	0.987	-9.9	11.5	14.6
Locarno-Monti	lo	r_lo_60min	8.787	46.173	370	-397.6	426.6	539.7	0.988	-10.6	11.4	14.4
Liepaja_rucava	lpj	r_lpj_60min	21.017	56.483	4	-366.6	380.1	461.2	0.991	-14.8	15.3	18.6
Lerwick	lrw	r_lrw_60min	-1.183	60.133	84	-206.9	308.0	393.4	0.982	-9.7	14.5	18.5
Sde Boqer	sbq	r_sbq_60min	34.767	30.767	457	-440.8	489.8	574.1	0.980	-8.6	9.6	11.3
Tartu_toravere	tar	r_tar_60min	26.466	58.265	70	-347.6	380.5	482.2	0.986	-14.0	15.3	19.4
Thessaloniki	ths	r_ths_60min	22.959	40.632	60	-361.2	504.7	654.2	0.968	-8.6	12.0	15.5
Bratislava	bai	r_bai_01min	17.071	48.169	195	-86.3	317.0	402.7	0.987	-2.9	10.7	13.6
Wroclaw	wri	r_wri_01min	17.014	51.126	111	-173.6	301.9	418.4	0.986	-6.1	10.6	14.7
Athens	ati	r_ati_01min	23.718	37.972	107	-241.7	323.6	403.5	0.988	-5.7	7.7	9.6
Ispra	isp	r_isp_01min	8.627	45.812	220	-162.9	262.4	332.4	0.993	-4.7	7.6	9.6
Vaulx un Velin	vix	r_vix_01min	4.922	45.779	170	-25.1	312.4	386.8	0.992	-0.7	9.3	11.5
Bergen	bei	r_bei_60min	5.332	60.384	45	-116.3	286.8	413.6	0.980	-6.1	15.1	21.7
Cimetta	ci	r_ci_10min	8.790	46.201	1670	-353.6	492.7	607.3	0.978	-9.6	13.3	16.4
Davos	da	r_da_60min	9.844	46.813	1610	-498.5	581.8	721.7	0.971	-13.6	15.8	19.6
Gornergrat	go	r_go_10min	7.785	45.984	3110	-1035.4	1116.6	1294.5	0.942	-22.7	24.5	28.4
SLF Versuchsfeld	vs	r_vs_10min	9.809	46.828	2540	-620.3	805.7	1008.4	0.927	-16.5	21.5	26.9
Weissfluhjoch	wf	r_wf_10min	9.805	46.833	2690	-646.1	833.0	1025.9	0.926	-17.1	22.1	27.2
Eggishorn	eg	r_eg_10min	8.927	46.427	2895	-564.3	1027.8	1255.9	0.868	-14.3	26.0	31.8
Jungfraujoch	jf	r_jf_60min	7.985	46.549	3580	-807.1	917.8	1155.8	0.941	-18.2	20.7	26.1

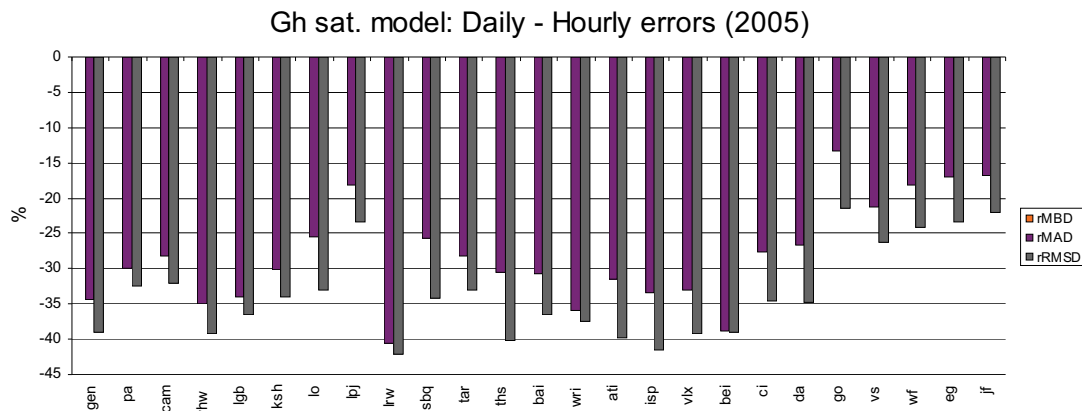


Fig. 6. Comparison of first order error measures for hourly and daily values $((E_d - E_h)/E_h) * 100\%$. Values represent error resolved by removing high frequency (hourly) error component

3.5. Monthly statistics of the satellite retrieval scheme performance

Accuracy measured calculated from monthly values of irradiation are still relatively high. rMAD and rRMSD decreased by removing daily variability. Most of the error is result of the high rMBD. For most of the stations rMBD is close in absolute terms to rMAD, it means negative bias for the all months of analyzed year.

Tab. 3: The summary results of the satellite retrieval scheme performance on monthly basis.

station	db	table	longitude	latitude	elev	MBD	MAD	RMSD	CC	rMBD	rMAD	rRMSD
Geneve	gen	r_gen_60min	6.132	46.200	420	-3.4	7.9	8.4	0.998	-3.4	8.0	8.5
Payerne	pa	r_pa_60min	6.943	46.814	490	-5.1	6.1	7.5	0.999	-6.1	7.3	9.0
Camborne	cam	r_cam_60min	-5.317	50.217	88	-9.0	9.0	10.1	0.997	-11.7	11.7	13.1
Wien_hohe_warte	whw	r_whw_60min	16.356	48.249	203	0.0	6.9	8.0	0.996	0.0	8.1	9.4
Loughborough	lgb	r_lgb_01min	-1.230	52.770	70	-3.2	5.2	6.2	0.996	-4.8	7.9	9.4
Kishinev	ksh	r_ksh_60min	28.816	47.001	205	-9.6	9.6	10.3	0.998	-11.0	11.0	11.9
Locarno-Monti	lo	r_lo_60min	8.787	46.173	370	-11.8	11.8	12.0	1.000	-11.9	11.9	12.1
Liepaja_rucava	lpj	r_lpj_60min	21.017	56.483	4	-10.4	10.4	11.7	0.995	-17.4	17.4	19.5
Lerwick	lrw	r_lrw_60min	-1.183	60.133	84	-6.3	6.7	7.9	0.995	-10.8	11.5	13.6
Sde Boqer	sbq	r_sbq_60min	34.767	30.767	457	-10.9	10.9	11.7	0.997	-9.5	9.5	10.1
Tartu_toravere	tar	r_tar_60min	26.466	58.265	70	-10.5	10.5	12.1	0.993	-16.3	16.3	18.8
Thessaloniki	ths	r_ths_60min	22.959	40.632	60	-9.8	9.8	11.3	0.996	-9.4	9.4	10.8
Bratislava	bai	r_bai_01min	17.071	48.169	195	-2.6	7.1	8.4	0.995	-3.0	8.2	9.7
Wroclaw	wri	r_wri_01min	17.014	51.126	111	-5.2	6.2	7.6	0.997	-6.5	7.8	9.6
Athens	ati	r_ati_01min	23.718	37.972	107	-7.3	7.3	8.6	0.999	-6.1	6.1	7.2
Ispra	isp	r_isp_01min	8.627	45.812	220	-4.9	5.6	6.5	1.000	-4.9	5.7	6.6
Vaulx un Velin	vlx	r_vlx_01min	4.922	45.779	170	-0.8	7.1	8.1	0.999	-0.8	7.0	8.0
Bergen	bei	r_bei_60min	5.332	60.384	45	-3.5	5.4	7.1	0.991	-6.5	10.1	13.4
Cimetta	ci	r_ci_10min	8.790	46.201	1670	-10.6	10.6	12.3	0.998	-10.6	10.6	12.3
Davos	da	r_da_60min	9.844	46.813	1610	-15.1	15.1	16.6	0.991	-15.7	15.7	17.3
Gornergrat	go	r_go_10min	7.785	45.984	3110	-31.2	31.2	32.6	0.986	-29.4	29.4	30.7
SLF Versuchsfeld	vs	r_vs_10min	9.809	46.828	2540	-18.6	21.4	25.0	0.939	-19.8	22.9	26.7
Weissfluhjoch	wf	r_wf_10min	9.805	46.833	2690	-19.4	22.4	25.8	0.937	-20.7	23.8	27.4
Eggishorn	eg	r_eg_10min	8.927	46.427	2895	-16.8	24.9	27.7	0.915	-16.7	24.8	27.5
Jungfrauoch	jf	r_jf_60min	7.985	46.549	3580	-23.7	23.7	25.7	0.985	-22.2	22.2	24.2

4. Conclusion

Within this paper, first results of a new scheme for solar irradiance retrieval from SEVIRI-MSG data have been discussed. Satellite model assessment has shown a general underestimation of the global solar irradiance compared with the ground measurements and an errors increase with site altitude.

References

- [1] Perez R., D. Renne, R. Seals, and A. Zelenka, (1998). The Strength of Satellite-based Solar Resource Assessment, Production of site/time-specific irradiances from satellite and ground data, Report 98-3, New York State Energy Research and Development Authority, Albany, NY.
- [2] D. Cano, J. Monget, M. Albuissou, H. Guillard, N. Regas, and L. Wald, Solar Energy, 37 (1984) 31–39.
- [3] A. Hammer, D. Heinemann, C. Hoyer, E. Lorenz, R.W. Müller, and H. Beyer, Remote Sensing of the Environment, 86 (2003) 423–432.
- [4] R. Pinker and I. Laszlo, J. of App. Meteorology, 31 (1994) 166–170.
- [5] R.W. Mueller, K.F. Dagestad, P. Ineichen, M. Schroedter-Homscheidt, S. Cros, D. Dumortier, et al., Remote Sensing of the Environment, 91 (2004) 160–174.

- [6] J. Verdebout, *J. Geophys. Res.*, 105 D4 (2000) 5049-5058.
- [7] B. Mayer and A. Kylling, *Atmos. Chem. Phys.*, 7 (2005) 1855-1877.
- [8] J. Polo, L.F. Zarzalejo, and L. Ramirez, “*Solar Radiation Derived from Satellite Images*” (Ch.18) in V. Badescu (Ed.), *Modeling Solar Radiation at the Earth Surface*. Springer-Verlag, 2008.
- [9] H. Georg Beyer et al. *Handbook on Benchmarking of Radiation Products*. Management and Exploitation of Solar Resource Knowledge (MESOR) Project – D1.1.3, EU FP6 Contract 038665, 2009.